

# Autoencoded UMAP-Enhanced Clustering for Unsupervised Learning

M. Chavooshi, A. V. Mamonov\*

Department of Mathematics, University of Houston, Houston, 77204-3008, TX, USA

## ARTICLE INFO

### Keywords:

Unsupervised machine learning  
Clustering  
Deep learning  
Convolutional autoencoder  
UMAP  
MNIST

## ABSTRACT

We propose a novel approach to unsupervised learning by constructing a non-linear embedding of the data into a low-dimensional space followed by any conventional clustering algorithm. The embedding promotes clusterability of the data and is comprised of two mappings: the encoder of an autoencoder neural network and the output of UMAP algorithm. The autoencoder is trained with a composite loss function that incorporates both a conventional data reconstruction as a regularization component and a clustering-promoting component built using the spectral graph theory. The two embeddings and the subsequent clustering are integrated into a three-stage unsupervised learning framework, referred to as Autoencoded UMAP-Enhanced Clustering (AUEC). When applied to MNIST data, AUEC significantly outperforms the state-of-the-art techniques in terms of clustering accuracy.

## 1. Introduction


Clustering is a fundamental tool in unsupervised machine learning, data mining and pattern recognition. However, it remains notoriously challenging when the underlying topology of the data manifold is complicated. Thus, the best clustering techniques are expected to include some form of manifold learning to gain an insight into the topological structure of the data before performing clustering itself. One possible approach to learn and simplify the topology of the data is to employ dimensionality reduction (DR) techniques prior to clustering. A large variety of such methods exists, ranging from basic ones such as the principal component analysis (PCA) to more advanced nonlinear DR approaches like Uniform Manifold Approximation and Projection (UMAP) Becht, McInnes, Healy, Dutertre, Kwok, Ng, Ginhoux and Newell (2019), Laplacian eigenmaps Belkin and Niyogi (2001), LargeVis Tang, Liu, Zhang and Mei (2016) and many more.

Deep neural networks (DNNs) Schmidhuber (2015) represent another class of techniques that is increasingly employed for DR before clustering. Examples include the stacked autoencoder (SAE) Vincent, Larochelle, Lajoie, Bengio, Manzagol and Bottou (2010), deep CCA (DCCA) Andrew, Arora, Bilmes and Livescu (2013), and sparse autoencoders Ng et al. (2011) that learn nonlinear mappings from the data domain to low-dimensional latent spaces. These approaches treat DNNs as a separate preprocessing stage from clustering, hoping that the latent representations learned will naturally be suitable for clustering. However, without

explicitly incorporating a clustering-promoting objective in the learning process, the resulting DNNs do not necessarily produce reduced-dimension data amenable to clustering. Thus, a number of recent works has explored merging DR with clustering rather than using DR merely as a preprocessing tool, e.g., Soete and Carroll (1994); Patel, Nguyen and Vidal (2013); Yang, Fu, Sidiropoulos and Hong (2017). These are the so-called unified approaches that optimize both deep representation learning and clustering objectives simultaneously. All of them are build on the assumption of the existence of a latent space where entities form distinct clusters. Therefore, it is logical to look for a DR transformation that unveils this structure, e.g., one that results in a small K-means loss function. This led to the idea of using the K-means cost function in the latent space to guide DR toward producing data representations amenable to K-means clustering.

Following the above considerations, a number of approaches was developed. For example, the so-called Deep Embedded Clustering (DEC) Xie, Girshick and Farhadi (2016) maps the observed space to a lower-dimensional latent space using SAE, simultaneously deriving feature representations and cluster assignments. Further improvements were later introduced in the form of Deep Clustering Network (DCN) Li, Qiao and Zhang (2018) that augments DEC by substituting SAE with a convolutional autoencoder (CAE), while IDEC Guo, Gao and Y. (2017) integrates the reconstruction loss of autoencoders into DEC's objective Xie et al. (2016). In all the approaches discussed above, the clustering module is linked to DNN's output, aiming for a simultaneous learning of both DNN parameters and cluster assignments. This leads to an optimization

\*Corresponding author.

 malihehsadat.chavooshi@bcm.edu (M. Chavooshi);  
avmamonov@uh.edu (A.V. Mamonov)

problem

$$\underset{w, \theta}{\text{minimize}} \sum_{i=1}^N q(f(x_i; w); \theta), \quad (1)$$

where  $f(x_i; w)$  is the output of the network given data instance  $x_i$ ,  $w$  contains the network weights, and  $\theta$  corresponds to parameters of a specific clustering model. For example, for K-means clustering  $\theta$  contains the centroids and cluster assignments. Here,  $q$  stands for a clustering loss, such as the Kullback–Leibler (KL) divergence loss featured in Xie et al. (2016) or the agglomerative clustering loss from Yang, Parikh and Batra (2016), possibly with regularization terms added to it.

While the approaches Yang et al. (2016); Xie et al. (2016); Li et al. (2018); Guo et al. (2017) proved a certain degree of effectiveness, there is still room for improvement. First, some improvement may be achieved from using an alternative clustering loss. Here we employ the spectral graph theory to derive such a loss. Second, one may notice that using DNN alone may be insufficient for learning an efficient representation of the data and therefore may lead to sub-optimal clustering results. Thus, we propose to augment DNN-based DR with a secondary DR step that utilizes the power of Uniform Manifold Approximation and Projection (UMAP) McInnes, Healy and Melville (2018) to refine the DNN embedding and further improve the clusterability of the embedded data. This results in a three-stage unsupervised learning framework that we refer to as Autoencoded UMAP-Enhanced Clustering (AUEC).

## 2. Autoencoded UMAP-Enhanced Clustering framework

We begin the discussion of AUEC with a brief description of each of its three stages.

### Stage I: Autoencoder with Joint loss

The first stage of AUEC is DR performed by means of embedding the data  $X = \{x_i\}_{i=1}^N$  into a latent space via an autoencoder-like DNN trained using a joint loss. We refer to this primary DR as the compressed embedding. The joint loss is given by a weighted sum of two components. First, is the component that measures the quality of clustering (clusterability) of the data embedded into the latent space. We refer to this component as the clustering loss. It can employ a variety of different clusterability measures as discussed below. Its purpose is to enforce a topology of the latent space that emphasizes the cluster structure of the data. Second, is the conventional reconstruction loss of an autoencoder. Its presence provides a regularization effect on

the network training by preventing trivial embeddings that may be produced by minimizing the clustering loss on its own. Thus, we refer to it as the regularization loss. The purpose of the first stage is to untangle the local cluster structure of the data. However, it may be insufficient to obtain the most optimal embedding for subsequent clustering. Therefore, it is followed by another DR stage.

### Stage II: Secondary DR via UMAP

To further enhance clusterability in the latent space, we follow the compressed embedding by a secondary DR step performed via UMAP McInnes et al. (2018). It is powerful nonlinear DR technique that combines the ideas of spectral clustering with those of Riemannian geometry Allaoui, Kherfi and Cheriet (2020). Its two key hyperparameters are the dimension of the output space  $n_C$  (the number of components) and the number of neighbors  $n_N$ , which controls the balance between local and global structure Kobak and Linderman (2021).

We refer to this secondary embedding as the refined embedding, since the purpose of the second stage is to further refine the latent representations to emphasize the global patterns in the embedded data thus making it more cluster-friendly. By applying UMAP after the compressed embedding we have the advantage of choosing DNN architecture based on the type of the data set. For example, for image data, a CAE presents the best choice. Therefore, interchanging the order of the first two stages is undesirable, since performing UMAP first leads to a loss of data structure that can be otherwise exploited with a particular choice of DNN architecture.

### Stage III: Clustering

After obtaining the compressed (Stage I) and refined (Stage II) embeddings of the data, any conventional clustering algorithm can be applied to categorize the embedded data. Note that the choice of a particular clustering algorithm is not required to be correlated with the clusterability measure used to train the DNN auto-encoder in Stage I. For example, choosing in Stage I as a clustering loss the cost function of K-means may be followed by DBSCAN in Stage III. This flexibility is made possible by the secondary DR in Stage II. Specifically, UMAP improves the overall clusterability of the refined embedding not just with respect to a single clusterability measure trained for in Stage I, but most likely with respect to other such measures as well.

We summarize the three-stage AUEC framework in Algorithm 1 with the corresponding data flow displayed in Figure 1. A Python implementation of AUEC is available at <https://github.com/mchavooshi/AUEC>

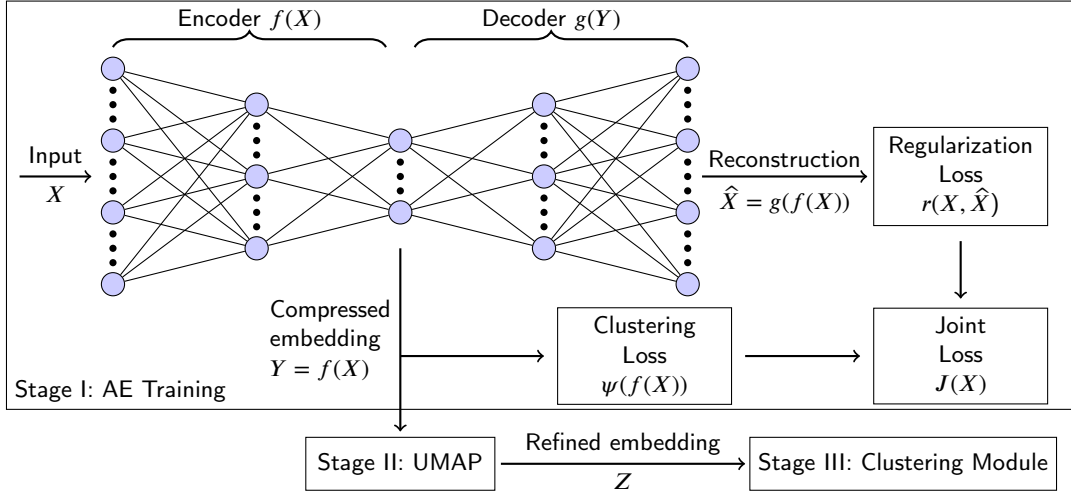


Figure 1: Data flow in AUEC.

### 3. Compressed embedding computation

We observe in Algorithm 1 that Stages II and III of AUEC consist of a straightforward application of standard algorithms to the compressed and refined embeddings of the data, respectively. On the other hand, computing the compressed embedding in Stage I is more involved and represents the bulk of the technical content of AUEC. In this section we discuss the computation of the compressed embedding in detail.

#### 3.1. Autoencoder and regularization loss

The main part of AUEC Stage I is training the autoencoder  $g(f(X; w_f); w_g)$ . Thus, the key step is to choose its architecture. As mentioned above, this choice should exploit fully the structure of the data. In this paper we illustrate the performance of AUEC with an example of a dataset of images, therefore it makes sense to employ a convolutional autoencoder (CAE). Specifically, for MNIST dataset one may choose a CAE architecture as in Figure 2. The CAE is trained using the joint loss (5) which requires defining both its components. We defer the discussion of the clustering loss to Section 3.2, while we choose for the regularization loss the most commonly used reconstruction loss in autoencoder training, the Mean Squared Error (MSE). The MSE loss measures the dissimilarity between the CAE output and the input, quantifying the reconstruction error as

$$\text{MSE}(X, \hat{X}) = \frac{1}{N} \sum_{i=1}^N \|x_i - \hat{x}_i\|_2^2. \quad (2)$$

Therefore, the regularization loss is defined by

$$\rho(X, g(f(X; w_f); w_g)) = \text{MSE}(X, g(f(X; w_f); w_g)). \quad (3)$$

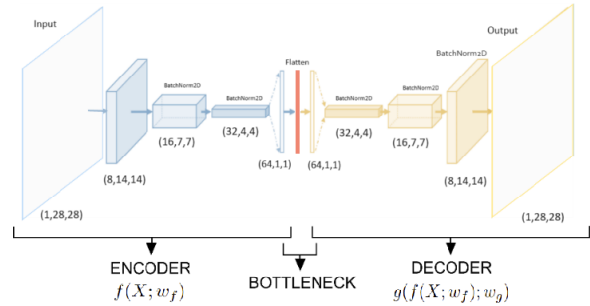


Figure 2: The architecture of the CAE used to work with image data. Convolutional layers are displayed in blue, while transposed convolutional layers are shown in yellow. The red layer in the middle represents the bottleneck, which flattens the data for latent space representation. Batch normalization is applied after each layer marked with "BatchNorm2D", and ReLU activation is used after each layer.

#### 3.2. Clustering loss

The main purpose of Stage I of AUEC is to produce a compressed embedding that is more clusterizable than the original data. This is achieved by the appropriate choice of the clustering loss in (5). Thus, we should employ as a clustering loss a function that promotes clusters with intra-cluster points being in close proximity while ensuring considerable distance between points in different clusters. Such functions are sometimes referred to as clusterability measures. The

**Algorithm 1** AUEC

- 1: **Input:** data set  $X = \{x_i\}_{i=1}^N \subset \mathbb{R}^M$ , the desired number of clusters  $K$ , UMAP hyper-parameters: number of components  $n_C$  and number of neighbors  $n_N$ .
- 2: **Stage I:** Train the autoencoder  $\hat{x}_i = g(f(x_i; w_f); w_g)$ , where

$$y_i = f(x_i; w_f), \quad i = 1, \dots, N, \quad (4)$$

is the encoder with weights  $w_f$ , and  $g(y_i; w_g)$  is the decoder with weights  $w_g$  and  $Y = \{y_i\}_{i=1}^N \in \mathbb{R}^m$  is the compressed embedding of the data with  $m \ll M$ . The training is performed by solving the optimization problem

$$\underset{w_f, w_g}{\text{minimize}} J(X, K; w_f, w_g)$$

where  $J$  is the joint loss of the form

$$J(X, K; w_f, w_g) = \lambda \psi\left(f(X; w_f), K\right) + \rho\left(X, g(f(X; w_f); w_g)\right). \quad (5)$$

Here  $\psi$  is the clustering loss,  $\rho$  is the regularization loss and  $\lambda > 0$  is the regularization parameter. Once the AE training is complete, compute the compressed embedding  $Y$  via (4) and pass it onto Stage II.

- 3: **Stage II:** Apply UMAP with hyper-parameters  $n_C$  and  $n_N$  to  $Y$  to obtain the refined embedding  $Z = \{z_i\}_{i=1}^N \subset \mathbb{R}^{n_C}$ , with  $n_C < m$ .
- 4: **Stage III:** Apply a clustering algorithm of choice to  $Z$  to obtain the clustering  $C(Z) = \{C_1, \dots, C_K\}$  of  $Z$ , where  $C_j \subseteq Z$ ,  $j = 1, \dots, K$ , with

$$Z = \bigsqcup_{j=1}^K C_j. \quad (6)$$

simplest and the most widely used such measure is the so-called within clusters sum of squares (WCSS) which is the loss function of K-means defined as

$$\text{WCSS}(Y, C(Y)) = \sum_{j=1}^K \sum_{y_i \in C_j} \left\| y_i - \frac{1}{|C_j|} \sum_{y_k \in C_j} y_k \right\|_2^2, \quad (7)$$

where  $C(Y) = \{C_1, \dots, C_K\}$  is the clustering of data  $Y$ . WCSS clusterability measure has been used before in the context of network training for unsupervised learning in Li et al. (2018); Yang et al. (2017). When used as a loss function for network training it has a disadvantage of requiring the data to be clustered

at each training iteration. This requires modifying the standard training procedures by splitting them into a part that updates the clustering assignment  $C(Y)$  which is then frozen and passed to the part that updates the network weights. In order to avoid these complications, we employ here as a clustering loss an alternative clusterability measure that is built using the spectral graph theory.

The central concepts of the spectral graph theory Chung (1997) are the graph-Laplacian matrix and its spectrum defined as follows. First, given the data  $Y$ , one constructs a similarity matrix  $\mathbf{S} \in \mathbb{R}^{N \times N}$  where each entry  $s_{ij}$  measures the similarity between  $y_i$  and  $y_j$ , while also setting  $s_{ii} = 0$ , e.g.,

$$s_{ij} = e^{-\gamma \|y_i - y_j\|^2}, \quad \gamma > 0. \quad (8)$$

Then, introducing the diagonal degree matrix  $\mathbf{D} \in \mathbb{R}^{N \times N}$  with entries  $d_{ii} = \sum_{j=1}^N s_{ij}$  one defines the normalized graph-Laplacian as

$$\mathbf{L} = \mathbf{I}_N - \mathbf{D}^{-\frac{1}{2}} \mathbf{S} \mathbf{D}^{-\frac{1}{2}}, \quad (9)$$

where  $\mathbf{I}_N$  is the identity matrix. Next, consider the eigenvalues of  $\mathbf{L}$  arranged in the non-decreasing order

$$0 = \lambda_1 \leq \lambda_2 \leq \dots \quad (10)$$

Classically, the spectral gap is the difference between its second smallest eigenvalue  $\lambda_2$  and its smallest eigenvalue  $\lambda_1 = 0$ :

$$\Delta \lambda_1 = \lambda_2 - \lambda_1 = \lambda_2. \quad (11)$$

A larger spectral gap signifies that the graph is well-connected. Conversely, a smaller or near-zero spectral gap suggests the presence of weak connections or potential bottlenecks in the graph. In the extreme case  $\gamma = \lambda_2 = 0$  the graph consists of two disconnected components.

When working with more than two clusters, one needs to generalize the spectral gap notion. This is motivated by the following spectral gap heuristic often used to decide how many clusters there are in the data von Luxburg (2007). If the data admits  $K$  well-defined clusters, one would expect the first  $K$  eigenvalues to be small, while  $\lambda_{K+1}$  should be relatively large. Similarly to the two clusters case, if the graph has  $K$  disconnected components, the zero eigenvalue appears  $K$  times with a noticeable gap before the next eigenvalue  $\lambda_{k+1} > 0$ . In general, the first eigenvalues of  $\mathbf{L}$  are related to the graph's topological properties like the sizes of graph cuts, see, e.g., Chung (1997).

Given the above, when classifying the data into  $K$  clusters, it is useful to consider consecutive eigenvalues of  $\mathbf{L}$ ,  $\lambda_{K+1}$  and  $\lambda_K$  and their differences

$$\Delta \lambda_K = \lambda_{K+1} - \lambda_K. \quad (12)$$

Since we are interested in constructing a loss function out of the spectral gap, it is more convenient for the purposes of optimization to work with the relative quantity

$$\text{RSG}(Y, K) = \frac{\lambda_{K+1}}{\lambda_K} = \frac{\Delta\lambda_K}{\lambda_K} + 1, \quad (13)$$

that we refer to as the relative spectral gap (RSG). Note that computing (13) does not require the data to be clustered. Maximizing this quantity has an enhancing effect on clustering the data into  $K$  clusters. Therefore, RSG can be used as a clusterability measure alternative to the conventional WCSS (7) with the higher values of RSG corresponding to better clustering results. This makes it a good candidate for a clustering loss that can be defined as

$$\psi(Y, K) = \frac{1}{\text{RSG}(Y, K)} \quad (14)$$

where  $Y = f(X; w_f)$ .

### 3.3. Autoencoder training

Once both the clustering loss and the regularization loss components of the joint loss (5) are fixed, the autoencoder can be trained using any off-the-shelf optimizer. The only part of AE training that requires special attention is the initial guess for the weights  $[w_f; w_g]$ . Given that the joint loss (5) is expressed as a sum of two terms, it makes sense to employ a simple pre-training technique consisting of training the AE network with just a regularization loss, i.e., setting  $\lambda = 0$  in (5) for a small number of epochs (e.g., we pre-train the AE for 5 epochs in the numerical experiments below).

## 4. Numerical experiments

In this section, we validate AUEC framework on MNIST dataset Lecun, Bottou, Bengio and Haffner (1998). The dataset consists of grayscale images, each depicting a handwritten digit. The size of each image is  $28 \times 28 = 784$  pixels. There are a total of 10 image classes corresponding to the numerical digits (0 to 9). The dataset is labeled, i.e., for each digit its ground truth class is known. Even though AUEC is an unsupervised learning framework, we use the available ground truth labels to measure the accuracy of the clustering it produces. The MNIST dataset consists of two subsets: a training set with 60,000 samples and a testing set with 10,000 samples. For the numerical experiments below we use  $N = 60,000$  samples from the training set.

### 4.1. Baseline Methods

We compare the performance of AUEC against a number of basic unsupervised learning approaches, as well as a few leading state-of-the-art techniques:

- (1) **KMS** is the baseline method that applies the K-means algorithm directly to raw image data.
- (2) **UMAP+KMS** utilizes UMAP to embed the images into a lower-dimensional space, after which K-means clustering is performed on the UMAP-embedded data.
- (3) **Deep Embedded Clustering (DEC)** of Xie et al. (2016) learns feature representations and determines cluster centers using deep AE and soft K-means, respectively. Similarly to Stage I of AUEC, the deep AE model is trained with a joint loss with the clustering loss taken as the Kullback–Leibler (KL) divergence.
- (4) **Deep Clustering Network (DCN)** of Yang et al. (2017) combines K-means clustering with DR via deep SAE similar to DEC. However, instead of KL divergence of DEC, DCN utilizes the WCSS loss as the clustering component of its joint loss.
- (5) **Fully Convolutional Autoencoder (FCAE)-KMS** of Li et al. (2018) is similar to DCN, but it adopts FCAE for image feature extraction.

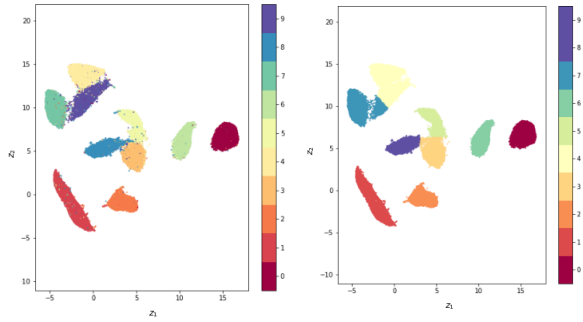
### 4.2. Results

The results of numerical experiments are presented below both numerically and visually. Numerically, we judge the performance of AUEC and other approaches via the three evaluation metrics discussed in Section 4.3. For visual evaluation of results, we rely on 2D embedding techniques, where appropriate. For the approaches involving UMAP (including AUEC itself), we rely on the embeddings it provides for  $n_C = 2$ . In all the 2D embeddings, we color-code the data points based on either their ground truth class labels or predicted cluster labels. This indicates the areas of agreement and disagreement between the ground truth classes and the predicted clusters.

#### 4.2.1. UMAP+KMS

Since UMAP is an integral part of the AUEC framework, it makes sense to study how it performs in a clustering setting while being the only DR transform applied to the data. We set UMAP hyper-parameters to  $n_N = 15$  and  $n_C = 2$  which corresponds to embedding the data into the 2D space for ease of visualization. After UMAP embedding we perform K-means and display the results in Figure 3. We observe that the digits “0”, “1”, “2” and “6” are well-separated and almost perfectly recovered by K-means from the embedded data. However, there are two three-digit clouds that are harder to classify. These are the “3-5-8” and “4-7-9” clouds. We observe in the predicted labels plot that while K-means did a decent job separating the “3-5-8” cloud into three clusters, it failed to do so with the “4-7-9” cloud. In fact, it was only able to identify two

clusters in that cloud instead of three and therefore only found 9 clusters in the UMAP-embedded data instead of 10.



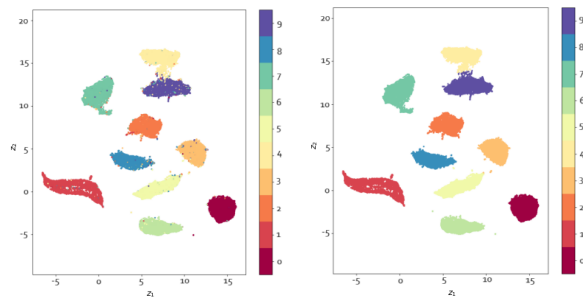
(a) Ground truth labels. (b) K-means predicted labels.

Figure 3: UMAP-embedded MNIST data.

#### 4.2.2. AUEC-MDBSCAN

We present here the results of applying AUEC to MNIST data with a special choice of clustering algorithm for Stage III. In particular, we utilize a modification of DBSCAN Ester, Kriegel, Sander, Xu et al. (1996) in which we enforce the output of  $K = 10$  clusters by merging the smaller clusters and outliers that DBSCAN produces with the 10 largest ones based on proximity. We refer to this variant of the framework as AUEC-MDBSCAN.

Similarly to the previous section, we display in Figure 4 the refined embedding  $Z$  of MNIST data computed by AUEC-MDBSCAN for  $n_C = 2$  and  $n_N = 5$ . Comparing the results to those in Figure 3 we observe an excellent separation of clusters. In particular, clusters “3” and “5” are now completely detached. All other digit classes are well-separated as well, except for a relatively thin neck connecting “4” and “9”.



(a) Ground truth labels. (b) AUEC-MDBSCAN labels.

Figure 4: AUEC-MDBSCAN refined embedding of MNIST data.

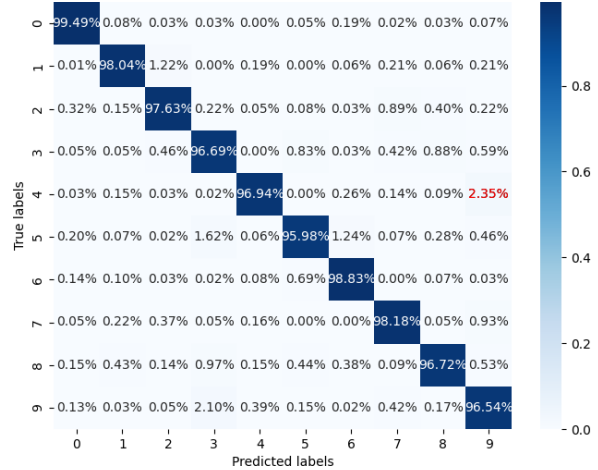


Figure 5: AUEC-MDBSCAN confusion matrix with the worst confusion shown in red.

To provide a deeper insight into the performance of AUEC-MDBSCAN we provide additional visualization in Figures 5 and 6. These visualizations no longer require  $n_C = 2$ , so in order to achieve the best possible performance we set  $n_C = 8$  with  $n_N = 6$ . In particular, in Figure 5 we display the confusion matrix showing the percentage of digits in the intersections of each ground truth and predicted classes. Ideally, the confusion matrix should be diagonal with 100% main diagonal entries and zero entries elsewhere. Any misclassified digits manifest themselves as non-zero off-diagonal entries with the largest such entry referred to as the worst misclassification. As expected from the results in Figure 4, we observe that the worst misclassification occurs for the classes “4” and “9” with 2.35% of ground truth “4” digits misclassified as “9”. A total of 137 such digits are displayed in Figure 6. Indeed, to a human eye many of these digits look like “9”. Visually, AUEC-MDBSCAN is vastly superior to UMAP+KMS which is also confirmed numerically in the next section.

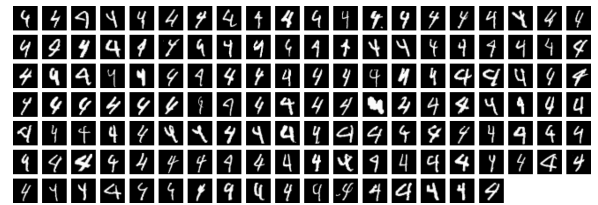


Figure 6: Digits corresponding to AUEC-MDBSCAN worst misclassification.

#### 4.3. Comparative Analysis

Here we compare AUEC to the other approaches listed in Section 4.1 using the standard metrics for

**Table 1**

Comparative performance of unsupervised learning methods on MNIST data.

Methods	ACC	NMI	ARI
KMS	59.07%	50.95%	40.47%
UMAP+KMS	86.59%	85.73%	80.41%
DEC	84.30%	-	-
DCN	83%	81%	75%
FCAE-KMS	79.4%	69.8%	-
<b>AUEC-MDBSCAN</b>	<b>97.52%</b>	<b>93.46%</b>	<b>94.64%</b>

assessing clustering performance. Specifically, we employ the three key metrics: normalized mutual information (NMI) Cai, He and Han (2010), adjusted Rand index (ARI) Yeung and Ruzzo (2001), and clustering accuracy (ACC) Cai et al. (2010). We summarize the testing results of Sections 4.2.1–4.2.2 in Table 1 while also comparing them to the results for DEC, DCN, and FCAE-KMS. The results for AUEC-MDBSCAN shown in Table 1 correspond to  $n_C = 8$  with  $n_N = 6$ .

We observe that AUEC vastly outperforms the existing approaches achieving an impressive accuracy of 97.5%. This is due to a powerful combination of AE and UMAP that AUEC employs. Indeed, UMAP by itself is such a powerful DR technique that simply combined with K-means it outperforms the DNN-based approaches from Xie et al. (2016); Yang et al. (2017); Li et al. (2018). Combining UMAP with an AE network trained with a carefully chosen clustering-promoting loss results in an even more powerful approach that is AUEC. In fact, when applied to MNIST dataset, AUEC-MDBSCAN scores fourth (as of August 2024) in terms of ACC in “Unsupervised Image Classification on MNIST” according to

<https://paperswithcode.com/sota/>

[unsupervised-image-classification-on-mnist](https://paperswithcode.com/sota/unsupervised-image-classification-on-mnist)

## Acknowledgments

A.M. and M.C. were supported by the U.S. National Science Foundation under awards DMS-1619821 and DMS-2309197. This material is based upon research supported in part by the U.S. Office of Naval Research under award number N00014-21-1-2370 to A.M.

## References

Allaoui, M., Kherfi, M.L., Cheriet, A., 2020. Considerably improving clustering algorithms using UMAP dimensionality reduction technique: A comparative study, in: International Conference on Image and Signal Processing, Springer. pp. 317–325.

Andrew, G., Arora, R., Bilmes, J., Livescu, K., 2013. Deep canonical correlation analysis, in: Proceedings of the 30th International Conference on Machine Learning, pp. 1247–1255.

Becht, E., McInnes, L., Healy, J., Dutertre, C.A., Kwok, I.W., Ng, L.G., Ginhoux, F., Newell, E.W., 2019. Dimensionality reduction for visualizing single-cell data using UMAP. *Nature Biotechnology* 37, 38–44.

Belkin, M., Niyogi, P., 2001. Laplacian eigenmaps and spectral techniques for embedding and clustering, in: *Advances in Neural Information Processing Systems*, pp. 585–591.

Cai, D., He, X., Han, J., 2010. Locally consistent concept factorization for document clustering. *IEEE Transactions on Knowledge and Data Engineering* 23, 902–913.

Chung, F.R.K., 1997. *Spectral graph theory*. American Mathematical Society.

Ester, M., Krieger, H.P., Sander, J., Xu, X., et al., 1996. A density-based algorithm for discovering clusters in large spatial databases with noise, in: *KDD*, pp. 226–231.

Guo, X., Gao, L., Y., X.L.J., 2017. Improved deep embedded clustering with local structure preservation, in: *International Joint Conference on Artificial Intelligence (IJCAI-17)*, pp. 1753–1759.

Kobak, D., Linderman, G.C., 2021. Initialization is critical for preserving global data structure in both t-SNE and UMAP. *Nature biotechnology* 39, 156–157.

Lecun, Y., Bottou, L., Bengio, Y., Haffner, P., 1998. Gradient-based learning applied to document recognition. *Proceedings of the IEEE* 86, 2278–2324. doi:10.1109/5.726791.

Li, F., Qiao, H., Zhang, B., 2018. discriminatively boosted image clustering with fully convolutional auto-encoders. *pattern recognition* 83, 161–173.

von Luxburg, U., 2007. A tutorial on spectral clustering. *Statistics and Computing* 17, 395–416.

McInnes, L., Healy, J., Melville, J., 2018. UMAP: Uniform manifold approximation and projection for dimension reduction. *arXiv preprint arXiv:1802.03426*.

Ng, A., et al., 2011. Sparse autoencoder. *CS294A Lecture notes* 72, 1–19.

Patel, V.M., Nguyen, H.V., Vidal, R., 2013. Latent space sparse subspace clustering, in: *Proceedings of the IEEE International Conference on Computer Vision*, pp. 225–232.

Schmidhuber, J., 2015. Deep learning in neural networks: An overview. *Neural networks* 61, 85–117.

Soete, G.D., Carroll, J.D., 1994. K-means clustering in a low-dimensional Euclidean space, in: *New Approaches in Classification and Data Analysis*, Springer. pp. 212–219.

Tang, J., Liu, J., Zhang, M., Mei, Q., 2016. Visualizing large-scale and high-dimensional data, in: *Proceedings of the 25th International Conference on World Wide Web*, pp. 287–297.

Vincent, P., Larochelle, H., Lajoie, I., Bengio, Y., Manzagol, P.A., Bottou, L., 2010. Stacked denoising autoencoders: Learning useful representations in a deep network with a local denoising criterion. *Journal of Machine Learning Research* 11.

Xie, J., Girshick, R., Farhadi, A., 2016. Unsupervised deep embedding for clustering analysis, in: *International Conference on Machine Learning*, PMLR. pp. 478–487.

Yang, B., Fu, X., Sidiropoulos, N.D., Hong, M., 2017. towards k-means-friendly spaces: simultaneous deep learning and clustering, in: *international conference on machine learning*, PMLR. pp. 3861–3870.

Yang, J., Parikh, D., Batra, D., 2016. joint unsupervised learning of deep representations and image clusters, in: *proceedings of the ieee conference on computer vision and pattern recognition*, pp. 5147–5156.

Yeung, K.Y., Ruzzo, W.L., 2001. Details of the adjusted rand index and clustering algorithms, supplement to the paper an empirical study on principal component analysis for clustering gene expression data. *Bioinformatics* 17, 763–774.